Colorimetric and Ratiometric Fluorescence Detection of HSO_3^- with a NIR Fluorescent Dye

Wenjie Liu
Zhengzhou University
Chenchen Yang
Zhengzhou University
Hongyan Zhang
Beijing Institute of Fashion Technology
Zhanxian Li
Zhengzhou University
Mingming Yu (yumm@zzu.edu.cn)
Zhengzhou University https://orcid.org/0000-0002-4081-7774

Research Article

Keywords: Colorimetric, ratiometric fluorescence, HSO3−, NIR fluorescent dye.

Posted Date: May 13th, 2021

DOI: https://doi.org/10.21203/rs.3.rs-502796/v1

Version of Record: A version of this preprint was published at Journal of Fluorescence on August 2nd, 2021. See the published version at https://doi.org/10.1007/s10895-021-02794-1.

Abstract

Bisulfite (HSO_3^-) has been widely used in food and industry, which has brought convenience to human life, but also seriously endangered human health. In this work, the probe PBI was designed and synthesized to detect bisulfite (HSO_3^-) through nucleophilic addition reaction. The probe PBI showed a selective reaction to HSO_3^- and can quantitatively detect HSO_3^-. At the same time, the color of the probe PBI changed significantly, which provided a simple method for the naked eye to identify HSO_3^-. Finally, it was successfully applied to the fluorescence imaging of HSO_3^- in living cells.

1 Introduction

In food, HSO_3^- can be used as a bleaching agent, preservative, and antioxidant [1 – 3]. HSO_3^- is a bleaching agent to improve food color and antibacterial effects, and widely used in food processing [4]. Then it can be used as a preservative to inhibit microbial activity and prevent food spoilage [5]. In terms of antioxidants, HSO_3^- can prevent or delay food oxidation, improve food stability and extend storage life [6]. As a large amount of HSO_3^- may cause tissue damage in individuals, it is necessary to strictly control the amount of HSO_3^- in food [7 – 9]. HSO_3^- is a reducing agent that plays the key role in industries such as dyes, papermaking, leather making, and chemical synthesis [10 – 13]. HSO_3^- can bleach cotton fabrics and organic substrate [14], treat chromium-containing waste water [15], and be used as an electroplating additive [16]. In the physiological system, HSO_3^- is mainly produced by the oxidation of cysteine and glutathione, and this process is mediated through reactive oxygen species (ROS) [17, 18]. Toxicological studies had shown that low concentrations (< 450 μM) of HSO_3^- have a significant promoting effect on the vasodilation of the cardiovascular system [19]. However, when the expression of HSO_3^- rises in the vivo, it can cause a series of diseases [20 – 23]. Therefore, it is of great significance to study new methods of HSO_3^- detection.

Some conventional analysis techniques for the detection of bisulfite have been developed, such as spectrophotometry [24, 25], chemiluminescence measurements [26, 27], chromatography [28], electrochemistry [29, 30], and phosphorimetry [31]. However, the detection process of these methods is more complicated, and some of them are not sensitive enough. So far, many fluorescent probes have been developed for the detection of HSO_3^-, because they have obvious advantages, including admirable sensitivity, in-situ detection ability and easy visualization with the naked eye [32 – 34]. These probes mainly react with HSO_3^- by using several kinds of reaction mechanisms. For example, the nucleophilic reaction with aldehydes [35], hydrogen bonding [36], and the nucleophilic addition reaction with the carbon-carbon double bond [37 – 38].

In this work, a new colorimetric and ratiometric fluorescent probe PBI for detecting HSO_3^- was designed based on the nucleophilic addition reaction (Scheme 1). Through experiments, the detection properties of

the probe PBI and its application in biological fluorescence imaging have been studied.

2 Experimental

Materials

4-Bromonaphthalene-1-carbonitrile, hydrazine hydrate, 2-methoxyethanol, 3-methyl-2-butanone, 3-aminophenol, 1-bromo-3-chloropropane, N,N-dimethylformamide, acetic ether, petroleum ether, dichloromethane, anhydrous ethanol, dimethyl sulfoxide, $NaHCO_3$, $POCl_3$, K_2CO_3, Na_2SO_4, NaF, NaCl, NaBr, NaI, $NaHSO_3$, NaOH, KCl, $CaCl_2$, $AlCl_3$, $ZnCl_2$, $SnCl_2$, $Pb(NO_3)_2$, CuCl, $CuCl_2$, $FeCl_2$, $FeCl_3$, $MgCl_2$, AgCl, $Ni(NO_3)_2$, $MnCl_2$, Na_3PO_4, Na_2HPO_4, NaH_2PO_4, $Co(NO_3)_2$, $Cd(NO_3)_2$, Na_2CO_3, $NaBF_4$, NaI, NaN_3, $Na_2C_2O_4$, $NaNO_2$, NaSCN, $NaNO_3$, $NaHSO_4$, Ala, Arg, Asp, Cys, Hcy, Gln, Glu, Gly, His, Ile, Leu, Met, Phe, Pro, Ser, Urea, Val.

Laboratory apparatus

Dual-beam UV-vis Spectrophotometer (TU-1901), Fluorospectrophotometer (F-4600), 400 M NMR spectrometer (AVIII HD 400), High-resolution mass spectrometer (IonSpec4.7), pH meter (PHS-2F), Rotary evaporator (RE-2000B), Electronic analytical balance (FA2004), Constant temperature magnetic stirrer (85 – 2), Vacuum drying oven (DZF-6020), Circulating water vacuum pump (SHB-3), Vacuum oil pump (2XZ-4), Digital camera (D3300), Portable UV analyzer (ZF-5).

The parameters of the solution in spectral tests

Configure the PBI with concentration of 1×10^{-3} mol/L (dissolved in DMSO). Remove 30 μL of PBI solution and add it to 3000 μL solution containing 2400 μL PBS and 600 μL DMSO, the final concentration of PBI in the test system was 1×10^{-5} mol/L.

The concentrations of anion ions, metal ions and small biomolecules used in the detection were 0.01 mol/L initially. The concentration of HSO_3^- was 0.05 mol/L.

Synthesis and methods

The synthetic route was shown in Scheme 1. Compound 3 was prepared according to previously reported method [39].

Synthesis of compound 1

4-Bromonaphthalene-1-carbonitrile (692.9 mg, 3 mmol) was dissolved in a mixed solution of hydrazine hydrate 80% (1.5 mL, 30 mmol) and 2-Methoxyethanol (25 mL), the resulting mixture was then heated to 125°C, and reacted under reflux for 8 h. After that, the solution was cooled, filtered with suction, and washed with ethanol to obtain the compound **1** (440 mg, 72.8%). ^{1}H NMR (600 MHz, DMSO-d_6): δ_H 8.57 (d, J = 8.2 Hz, 1H), 8.41 (s, 1H), 8.16 (d, J = 8.0 Hz, 1H), 7.84–7.74 (m, 2H), 2.43 (s, 3H), 1.38 (s, 6H). ^{13}C

NMR (151 MHz, DMSO-d_6): δ_C 195.00, 152.79, 142.04, 133.14, 129.18, 128.26, 127.97, 125.92, 125.07, 124.41, 118.76, 105.43, 55.75, 22.10, 16.19.

Synthesis of compound 2

Compound **1** (402.75 mg, 2.2 mmol) was added to 3-methyl-2-butanone (20 mL), then concentrated sulfuric acid (0.5 mL) was mixed to get a white turbid liquid. The mixture was heated up to 125°C and reacted for 8 h. After the reaction, the mixture was cooled to room temperature, a solid precipitated out, and suction filtration to get the compound **2** (310 mg, 60.2%). ^{1}H NMR (400 MHz, DMSO-d_6): δ_H 8.61 (s, 1H), 8.26 (d, J = 8.5 Hz, 1H), 7.90 (dd, J = 19.5, 8.2 Hz, 2H), 7.71–7.63 (m, 1H), 7.55–7.46 (m, 1H), 7.07 (d, J = 8.3 Hz, 1H), 4.48 (s, 2H). ^{13}C NMR (151 MHz, DMSO-d_6): δ_C 151.91, 135.49, 133.43, 128.93, 125.62, 124.84, 122.86, 120.78, 120.27, 102.89, 93.4.

Synthesis of PBI

Compound **2** (217.11 mg, 1 mmol) and compound **3** (234.11 mg, 1 mmol) were dissolved in ethanol (30 mL), and the reaction mixture was heated to reflux for 12 h. Then the resulting mixture was cooled to room temperature and the product was collected by suction, washed with ethanol, and dried in vacuo (207.9 mg, 48.0%). ^{1}H NMR (400 MHz, DMSO-d_6): δ_H 8.64 (d, J = 7.7 Hz, 1H), 8.55 (s, 1H), 8.39 (s, 1H), 8.14 (d, J = 7.9 Hz, 1H), 7.94–7.73 (m, 2H), 7.52 (s, 1H), 7.00–6.85 (m, 1H), 3.37 (s, 5H), 2.77–2.55 (m, 4H), 1.89 (s, 4H), 1.57 (s, 6H). ^{13}C NMR (151 MHz, DMSO-d_6): δ_C 133.37, 129.58, 127.98, 125.24, 124.38, 118.99, 103.25, 50.03, 27.15, 25.10, 21.59, 21.24, 20.59, 15.61, 0.57.

3 Results And Discussion

Detection properties of probe PBI

For better experimental results, we must first select the most suitable experimental system. The DMSO content was changed from 10%, 20%, to 60% in the test system, and HSO_3^- was added to test under the same conditions. From Fig. 1a, when the DMSO content increased from 10–60%, the I_{397}/I_{646} decreased. The I_{397}/I_{646} reached the maximum as the DMSO content was 10%, but in comparison, when the DMSO content was 20%, the $\Delta I_{397}/I_{646}$ was the largest before and after the reaction. So we chose the test system as V_{water}:V_{DMSO}=8:2.

In order to understand the properties of fluorescent probe, it is very important to keep the properties of probe stable. As shown in Fig. 1b, The I_{397}/I_{646} showed a stable trend within 60 min, and the fluctuation range could be ignored. It indicated that the probe will not be disturbed by the illumination time, and showed good light stability.

For a better understanding of the practical application of the probe, the detection time of HSO_3^- with PBI was studied. Different concentrations of HSO_3^- (0 mmol/L, 0.2 mmol/L, 0.3 mmol/L, 0.4 mmol/L) were

added to the fluorescent probe PBI solution, and the fluorescence spectra were tested with reaction time changing. It can be seen from Fig. 1.c that when 0.2 mmol/L and 0.3 mmol/L HSO_3^- were added respectively, the I_{397}/I_{646} increased quickly in the first 12 min, and then reached the maximum when the time was 60 min. when 0.4 mmol/L HSO_3^- was added, the I_{397}/I_{646} increased rapidly and the reaction almost finished within 60 min. such results indicates that concentration of HSO_3^- can affect the detection rate at the first period and have no influence on the overall reaction time of probe with HSO_3^-.

The probe should have a wide range of pH for better detection of HSO_3^-. Test system separately was prepared with DMSO and deionized water of different pH, the pH ranges from 1 to 14, and fluorescence intensity of probe PBI was recorded in the absence and presence of HSO_3^-. As shown in Fig. 1d, in the pH range of 4 to 8, great difference of the I_{397}/I_{646} of probe PBI with and without HSO_3^- was obtained, so the optimal pH test range for the probe PBI to detect HSO_3^- was 4–8. Such result illustrated that probe PBI can detect HSO_3^- in a wide pH range and have potential applications in real sample detection.

The UV–vis spectral response of probe PBI to HSO_3^- was tested firstly. As shown in Fig. 2a, probe PBI showed the absorption maximum at 520 nm originally. Upon addition of HSO_3^- to the solution, the absorption peak at 520 nm gradually decreased, and the absorption peak progressively increased at 350 nm. When the HSO_3^- concentration in the test system was 0.07 mmol/L − 0.22 mmol/L, the A_{350}/A_{520} showed a good linear relationship with the HSO_3^- concentrations (Fig. 2b), this means that in this interval, we can achieved quantitative detection of HSO_3^-. After adding HSO_3^-, the color of PBI solution changed from pink to colorless under daylight (Fig. 2c), the change was so obvious that it provides an easy way to detect HSO_3^- with the naked eye.

Fluorescence spectra of probe PBI over various concentrations of HSO_3^- were recorded. As for PBI, We used double excitation mode that was to choose 350 nm and 520 nm as the excitation wavelength. As shown in Fig. 3a, after the titration of HSO_3^-, the fluorescence intensity of PBI at 392 nm increased gradually, while fluorescence intensity of PBI progressively decreased at 646 nm. In order to more directly express the relationship between fluorescence intensity and concentration of HSO_3^-, the I_{397}/I_{646} was plotted as a function of the concentration of HSO_3^- (Fig. 3b). In the range of 0.04 mmol/L − 0.19 mmol/L, the linear increase of I_{397}/I_{646} could be used in the quantitative detection of HSO_3^-. Upon addition of HSO_3^-, The color also changed significantly under portable UV lamps, gradually changing from pink to blue purple (Fig. 3c), which can be more convenient for HSO_3^- detection in practical applications.

Selectivity and anti-interference ability studies of probe PBI

The special selectivity of fluorescent probes for analytes was higher than other substances is an important feature of it. To understand the selectivity of probe PBI toward HSO_3^-, we conducted a series of controlled experiments with anions. As can be seen from Fig. 4, The A_{350}/A_{520} and I_{397}/I_{646} with only the

above anions added had no big difference compared with that of probe PBI only except HSO_3^-, which showed all these anions could not respond to probe PBI. The above anions and HSO_3^- were added to probe PBI solution at the same time, The A_{350}/A_{520} and I_{397}/I_{646} were significantly increased compared with that of probe PBI only. Obviously, probe PBI responds to HSO_3^- only, and when other anions and HSO_3^- coexist, there was no interference on the detection of HSO_3^- with probe PBI.

Meanwhile, similar to the above method, the influence of metal ions (Fig. S1) and amino acids (Fig. S2) on the detection of HSO_3^- with probe PBI was also explored. From the figures S1 and S2, it is clear that probe PBI can specifically select HSO_3^- in the presence of cations and amino acids, and thus probe PBI had good selectivity and strong anti-interference ability.

The reaction mechanism of probe to detect HSO_3^-

The reaction mixture of PBI and $NaHSO_3$ was analyzed by ESI-MS spectroscopy to explore the recognition mechanism of probe PBI to HSO_3^-. As shown in Fig. S3, m/z = 516.1957 (theoretical molecular weight = 516.1952) $[M + HSO_3 + H]^+$ was the peak after the carbon-carbon double bond nucleophilic addition reaction between probe PBI and HSO_3^-. So we proposed the detection mechanism of probe PBI for HSO_3^-: in the condition of HSO_3^-, six-membered ring of probe PBI was broken, and HSO_3^- was added to the position of the original carbon-carbon double bond (Scheme 1).

The detection of HSO_3^- in living cells

In order to explore the potential application of probe PBI in the detection of HSO_3^- in living cells, fluorescence confocal imaging experiments were performed in HeLa cells with probe PBI, and the images were captured under a confocal fluorescence microscope. We studied the feasibility of the probe PBI to detect exogenous HSO_3^- in HeLa cells. The bright field pictures showed the position in the living cells (Fig. 5a, 5d). The sole probe PBI emitted clear red fluorescence (Fig. 5b), when the cells were treated with HSO_3^-, the red fluorescence disappeared (Fig. 5e), and they overlaid well (Fig. 5c, 5f). The results indicated that probe PBI can effectively detect exogenous HSO_3^-, which can be used to detect HSO_3^- in the living cells.

Comparison of probe PBI with some reported probes toward HSO_3^-

As shown in Table 1, in terms of excitation wavelength/emission wavelength, detection medium, response type, pH, detection limit and cell application, probe PBI had good analytical performance compared with other HSO_3^- fluorescent probes reported recently.[40–45] The result showed that probe PBI was a ratiometric fluorescent probe with a low detection limit (208 nmol/L). Moreover, biological experiments have demonstrated the application of probe PBI in monitoring intracellular HSO_3^-.

Table 1

Comparison of various fluorescent probes for HSO_3^- detection.

Probe	$\lambda_{ex}/\lambda_{em}$ (nm)	Detection media	Response type	pH range	LOD	Cellular applications	Ref
PPA	395 455/604	DMSO/PBS (1:9, v/v)	ratiometric	7 – 9	11.03 μM	exogenous/ endogenous	40
probe 1	440/558 493/593	DMSO/HEPES (1:9, v/v)	off-on	4 – 8	0.87 μM	exogenous	41
EIM	440 476/579	PBS	ratiometric	5 – 11	0.20 μM	exogenous	42
BIQ	380/460 475/625	DMSO/H_2O (3:7, v/v)	ratiometric	4 – 11	0.29 μM	exogenous	43
probe 2	525 600	DMSO/PBS (5:5, v/v)	on-off	5 – 11	2.01 μM	exogenous	44
probe 1	366 420/530	Water/Ethanol (9:1, v/v)	ratiometric	Not good	0.77 μM	exogenous/ endogenous	45
PBI	350/520 397/646	DMSO/PBS (2:8, v/v)	ratiometric	4 – 8	208 nM	exogenous	This work

4 Conclusion

In summary, we have developed a new colorimetric and ratiometric fluorescence probe PBI to detect HSO_3^-. The reaction mechanism of probe PBI to detect HSO_3^- was attributed to the nucleophilic addition reaction. When the probe was added with HSO_3^-, the absorption and fluorescence emission changed significantly, and the color change was so obvious that it provided an easy way to detect HSO_3^- with the naked eye. In addition, probe PBI shows good selectivity and strong anti-interference ability for HSO_3^-. The probe PBI can in HeLa cells, which would be potential candidates to track HSO_3^- in live cells.

Declarations

Acknowledgements

We are grateful for the financial support from the National Natural Science Foundation of China (U1704161, U1504203 and 21601158) and Zhengzhou University (32210431).

Funding This work was supported by the National Natural Science Foundation of China (U1704161, U1504203 and 21601158) and Zhengzhou University (32210431).

Conflicts of interest/Competing interests The authors declare that they have no conflict of interest.

Ethics approval Not applicable.

Consent to participate Not applicable.

Consent for publication Not applicable.

Availability of data and material All data generated or analysed during this study are included in this published article and its supplementary information files.

Code availability All data were obtained using word, origin and chemBioDraw.

Authors' contributions All authors contributed to the study conception and design. Material preparation, data collection and analysis were performed by Wenjie Liu, Chenchen Yang and Hongyan Zhang. Fundings were acquired by Zhanxian Li and Mingming Yu. The first draft of the manuscript was written by Wenjie Liu, all authors commented on previous versions of the manuscript and the manuscript was revised by Zhanxian Li and Mingming Yu. All authors read and approved the final manuscript.

References

1. Lin VS, Chen W, Xian M, Chang CJ (2015) Chemical probes for molecular imaging and detection of hydrogen sulfide and reactive sulfur species in biological systems. Chem Soc Rev 44:4596–4618
2. Singha S, Jun YW, Sarkar S, Ahn KH (2019) An endeavor in the reaction-based approach to fluorescent probes for biorelevant analytes: challenges and achievements. Acc Chem Res 52:2571–2581
3. Ci Q, Qin X, Liu J, Wang R, Li Z, Qin W, Lim K-L, Zhang C-W, Li L (2020) Mitochondria-targeted polydopamine nanoprobes for visualizing endogenous sulfur dioxide derivatives in a rat epilepsy model. Chem Commun 56:11823–11826
4. Tamima U, Santra M, Song CW, Reo YJ, Ahn KH (2019) A benzopyronin-based two-photon fluorescent probe for ratiometric imaging of lysosomal bisulfite with complete spectral separation. Anal Chem 91:10779–10785
5. Zeng R-F, Lan J-S, Wu T, Liu L, Liu Y, Ho RJY, Ding Y, Zhang T (2020) A novel mitochondria-targetted near-infrared fluorescent probe for selective and colorimetric detection of sulfite and its application in vitro and vivo. Food Chem 318:1914–1921
6. Zhang W, Liu T, Huo F, Ning P, Meng X, Yin C (2017) Reversible ratiometric fluorescent probe for sensing bisulfate/H_2O_2 and its application in zebrafish. Anal Chem 89:8079–8083

7. Everitt KR, Schmitz HC, Macke A, Shan J, Jang E, Luedtke BE, Carlson KA, Cao H (2020) Investigation of a sensing strategy based on a nucleophilic addition reaction for quantitative detection of bisulfite (HSO_3^-). J Fluoresc 30:977–983
8. Gao C, Tian Y, Zhang R, Jing J, Zhang X (2019) Mitochondrial directed ratiometric fluorescent probe for quantitive detection of sulfur dioxide derivatives. New J Chem 43:5255–5259
9. Han X, Zhai Z, Yang X, Zhang D, Tang J, Zhu J, Zhu X, Ye Y (2020) A FRET-based ratiometric fluorescent probe to detect cysteine metabolism in mitochondria. Org Biomol Chem 18:1487–1492
10. He X, Xu W, Ding F, Xu C, Li Y, Chen H, Shen J (2020) Reaction-based ratiometric and colorimetric chemosensor for bioimaging of biosulfite in live cells, zebrafish, and food samples. J Agric Food Chem 68:11774–11781
11. Dutta T, Chandra F, Koner AL (2018) A rapid, naked-eye detection of hypochlorite and bisulfite using a robust and highly-photostable indicator dye Quinaldine Red in aqueous medium. Spectrochim Acta Part A 191:217–220
12. Bi K, Tan R, Hao R, Miao L, He Y, Wu X, Zhang J, Xu R (2019) A carbazole-hemicyanine dye based ratiometric fluorescent probe for selective detection of bisulfite (HSO3-) in cells and C. elegans. Chin Chem Lett 30:545–548
13. Gao H, Qi H, Peng Y, Qi H, Zhang C (2018) Rapid "turn-on" photoluminescence detection of bisulfite in wines and living cells with a formyl bearing bis-cyclometalated Ir(III) complex. Analyst 143:3670–3676
14. Nie J, Sun H, Zhao Y, Dai X, Ni Z (2021) An efficient hemicyanine dyes-based ratiometric fluorescence probe for sulfur dioxide derivatives in live-cells and seawater. Spectrochim Acta Part A 247:119–128
15. Pan X, Cheng S, Zhang C, Qi X (2020) Two highly sensitive fluorescent probes based on cinnamaldehyde with large Stokes shift for sensing of HSO_3^- in pure water and living cells. Anal Bioanal Chem 412:6959–6968
16. Guo S, Liu G, Fan C, Pu S (2018) A highly selective fluorescent probe for detection of Cd^{2+} and HSO_3^- based on photochromic diarylethene with a triazole-bridged coumarin-quinoline group. RSC Adv 8:22786–22798
17. Shi J, Shu W, Tian Y, Wu Y, Jing J, Zhang R, Zhang X (2019) A real-time ratiometric fluorescent probe for imaging of SO_2 derivatives in mitochondria of living cells. RSC Adv 9:22348–22354
18. Li X, Jin D, Du Y, Liu Y, Wang B, Chen L (2018) Several fluorescent probes based on hemicyanine for the detection of SO_2 derivatives. Anal Methods 10:4695–4701
19. Li Y, Ban Y, Wang R, Wang Z, Li Z, Fang C, Yu M (2020) FRET-based ratiometric fluorescent detection of arginine in mitochondrion with a hybrid nanoprobe. Chin Chem Lett 31:443–446
20. Lu J, Wu P, Geng Y, Wang J (2018) A simple and highly selective 1,2,4,5-tetrazine-based colorimetric probe for HSO_3^- ion recognition in food. RSC Adv 8:33459–33463
21. Wu L, Chen L, Kou M, Dong Y, Deng W, Ge L, Bao H, Chen Q, Li D (2020) The ratiometric fluorescent probes for monitoring the reactive inorganic sulfur species (RISS) signal in the living cell.

Spectrochim Acta Part A 231:118–141

22. Wu L, Qi S, Liu Y, Wang X, Zhu L, Yang Q, Du J, Xu H, Li Y (2021) A novel ratiometric fluorescent probe for differential detection of HSO_3^- and ClO^- and application in cell imaging and tumor recognition. Anal Bioanal Chem 413:1137–1148
23. Yan Y-H, Wu Q-R, Che Q-L, Ding M-M, Xu M, Miao J-Y, Zhao B-X, Lin Z-M (2020) A mitochondria-targeted fluorescent probe for the detection of endogenous SO_2 derivatives in living cells. Analyst 145:2937–2944
24. Paul S, Ghoshal K, Bhattacharyya M, Maiti DK (2017) Detection of HSO_3^-: A rapid colorimetric and fluorimetric selective sensor for detecting biological SO_2 in food and living cells. ACS Omega 2:8633–8639
25. Yang D, He X-Y, Wu X-T, Shi H-N, Miao J-Y, Zhao B-X, Lin Z-M (2020) A novel mitochondria-targeted ratiometric fluorescent probe for endogenous sulfur dioxide derivatives as a cancer-detecting tool. J Mater Chem B 8:5722–5728
26. Yang X, Yang Y, Zhou T, Jin M, Jing X, Miao CH, Li W (2019) A mitochondria-targeted ratiometric fluorescent probe for detection of SO2 derivatives in living cells and in vivo. J Photoch Photobio A 372:212–217
27. Pan X, Zhong Y, Jiang Y, Zuo G, Li J, Dong W (2018) Reaction-based fluorescent sensor for detection of bisulfite through 1,4-addition reaction in water. Mater Chem Phys 213:83–88
28. Zeng L, Chen T, Chen B-Q, Yuan H-Q, Sheng R, Bao G-M (2020) A distinctive mitochondrion-targeting, in situ-activatable near-infrared fluorescent probe for visualizing sulfur dioxide derivatives and their fluctuations in vivo. J Mater Chem B 8:1914–1921
29. Song G-J, Luo J, Xing X-j, Ma H-L, Yang D, Cao X-Q, Ge Y-Q, Zhao B-X (2018) A ratiometric fluorescence probe for rapid detection of mitochondrial SO_2 derivatives. New J Chem 42:3063–3068
30. Wang R, Wang R, Ju D, Lu W, Jiang C, Shan X, Chen Q, Sun G (2018a) "ON-OFF-ON" fluorescent probes based on nitrogen-doped carbon dots for hypochlorite and bisulfite detection in living cells. Analyst 143:5834–5840
31. Zheng X-L, Li H, Feng W, Xia H-C, Song Q-H (2018) Two-Step Sensing, Colorimetric and Ratiometric Fluorescent Probe for Rapid Detection of Bisulfite in Aqueous Solutions and in Living Cells. ACS Omega 3:11831–11837
32. Wang S-J, Li J, Gao Y, Guo Y (2018b) Highly selective and sensitive 2-(2 '-hydroxyphenyl)benzothiazole-based turn-on fluorescent probes for detecting and imaging bisulfite in living cells. Asian J Org Chem 7:563–569
33. Zhou F, Feng H, Li H, Wang Y, Zhang Z, Kang W, Jia H, Yang X, Meng Q, Zhang R (2020) Red-emission probe for ratiometric fluorescent detection of bisulfite and its application in live animals and food samples. ACS Omega 5:5452–5459
34. Zhou F, Sultanbawa Y, Feng H, Wang Y-L, Meng Q, Wang Y, Zhang Z, Zhang R (2019) A new red-emitting fluorescence probe for rapid and effective visualization of bisulfite in food samples and live

animals. J Agric Food Chem 67:4375–4383

35. Zhu J-L, Xu Z, Yang Y, Xu L (2019) Small-molecule fluorescent probes for specific detection and imaging of chemical species inside lysosomes. Chem Commun 55:6629–6671
36. Yang S, Wen X, Yang X, Li Y, Guo C, Zhou Y, Li H, Yang R (2018) Visualizing endogenous sulfur dioxide derivatives in febrile-seizure-induced hippocampal damage by a two-photon energy transfer cassette. Anal Chem 90:14514–14520
37. Yang Y, Zhou T, Bai B, Yin C, Xu W, Li W (2018) Design of mitochondria-targeted colorimetric and ratiometric fluorescent probes for rapid detection of SO_2 derivatives in living cells. Spectrochim Acta Part A 196:215–221
38. Zou L, Zhang G, Zhou M, Xin X, Chen S, Duan X, Xu J (2019) Two reaction-based fluorescent sensors with cationic group enable high-selective detection of HSO_3^- in the environment. Ind Eng Chem Res 58:9231–9238
39. Zhang Y, Teng H, Gao Y, Afzal MW, Tian J, Chen X, Tang H, James TD, Guo Y (2020) A general strategy for selective detection of hypochlorous acid based on triazolopyridine formation. Chin Chem Lett 31:2917–2920
40. Wang W, Li N, Liu J-T, Miao J-Y, Zhao B-X, Lin Z-M (2020) A new FRET-based ratiometric fluorescent probe for the detection of SO_2 derivatives in mitochondria of living cells. Dyes Pigments 181:108639
41. Yang Y, Bai B, Xu W, Xu Z, Zhang J, Li W (2017) A highly sensitive fluorescent probe for the detection of bisulfite ion and its application in living cells. Dyes Pigments 136:830–835
42. Zhao M, Liu D, Zhou L, Wu B, Tian X, Zhang Q, Zhou H, Yang J, Wu J, Tian Y (2018) Two water-soluble two-photon fluorescence probes for ratiometric imaging endogenous SO2 derivatives in mitochondria. Sensor Actuat B 255:1228–1237
43. Zhou F, Feng H, Li H, Wang Y, Zhang Z, Kang W, Jia H, Yang X, Meng Q, Zhang R (2020b) Red-Emission Probe for Ratiometric Fluorescent Detection of Bisulfite and Its Application in Live Animals and Food Samples. ACS Omega 5:5452–5459
44. Zhang L, Wang L, Zhang X, Zhu Z-J (2020) A colorimetric and fluorescent probe for sulfite/bisulfite based on conjugated benzothiazole derivative and imaging application in living cells. J Photoch Photobio A 395:112498
45. Chao J, Wang X, Liu Y, Zhang Y, Huo F, Yin C, Zhao M, Sun J, Xu M (2018b) A pyrene-thiophene based fluorescent probe for ratiometric sensing of bisulfite and its application in vivo imaging. Sensor Actuat B 272:195–202

Figures

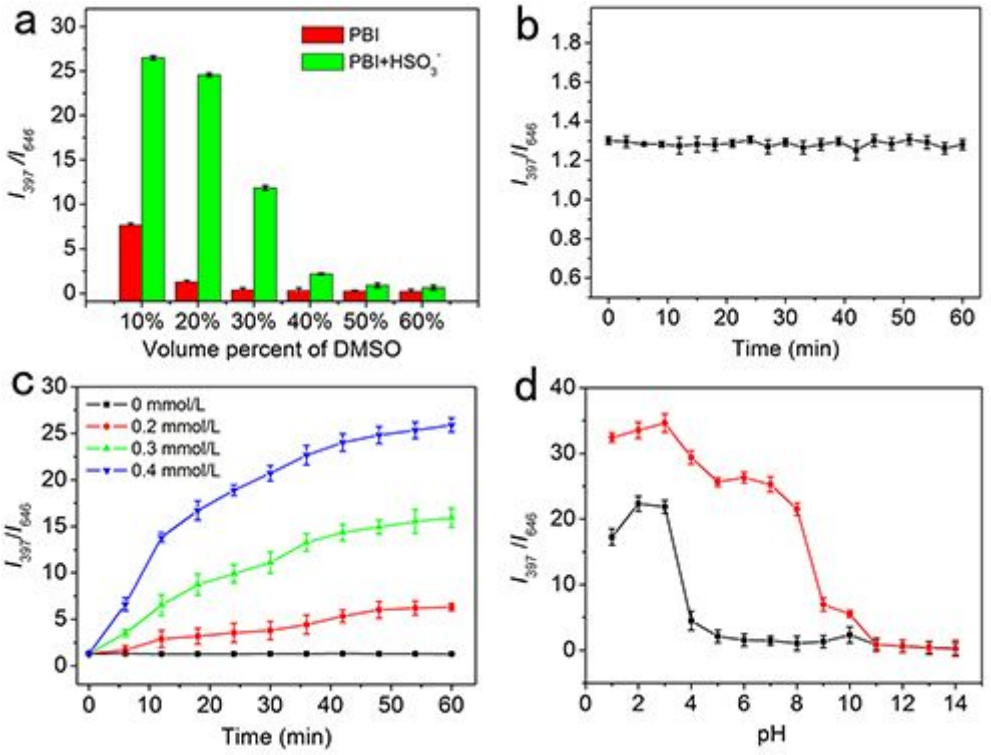

Figure 1

(a) The fluorescence intensity ratio I393/I646 of probe PBI (1×10−5 M) changes before (red column) and after (green column) adding HSO3− (0.4 mmol/L) to the system with different content of DMSO. (b) The fluorescence intensity ratio I393/I646 of probe PBI (1×10−5 M, Vwater:VDMSO = 8:2) as irradiation time changes. (c) Real-time records for I393/I646 changes of PBI with different concentrations of HSO3−. (d) The fluorescence intensity ratio I393/I646 of probe PBI in the absence (black) and presence (red) of HSO3− (0.4 mmol/L) at different pH (λex = 350 nm, 520 nm).

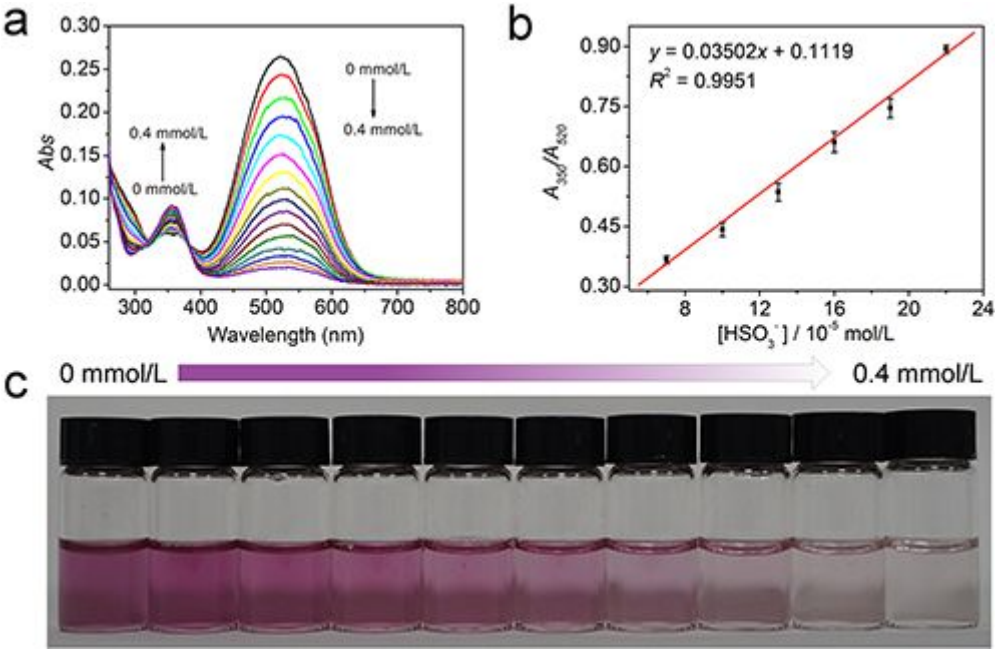

Figure 2

(a) UV–vis absorbance spectra of probe PBI (1×10−5 M, Vwater:VDMSO = 8:2) with various concentrations of HSO3− (0 mmol/L−0.4 mmol/L). (b) A350/A520 as a function of different concentrations of HSO3− (0.07 mmol/L−0.22 mmol/L). (c) Photographs of PBI (1×10−5 M, Vwater:VDMSO = 8:2) in the different concentrations of HSO3− under natural light.

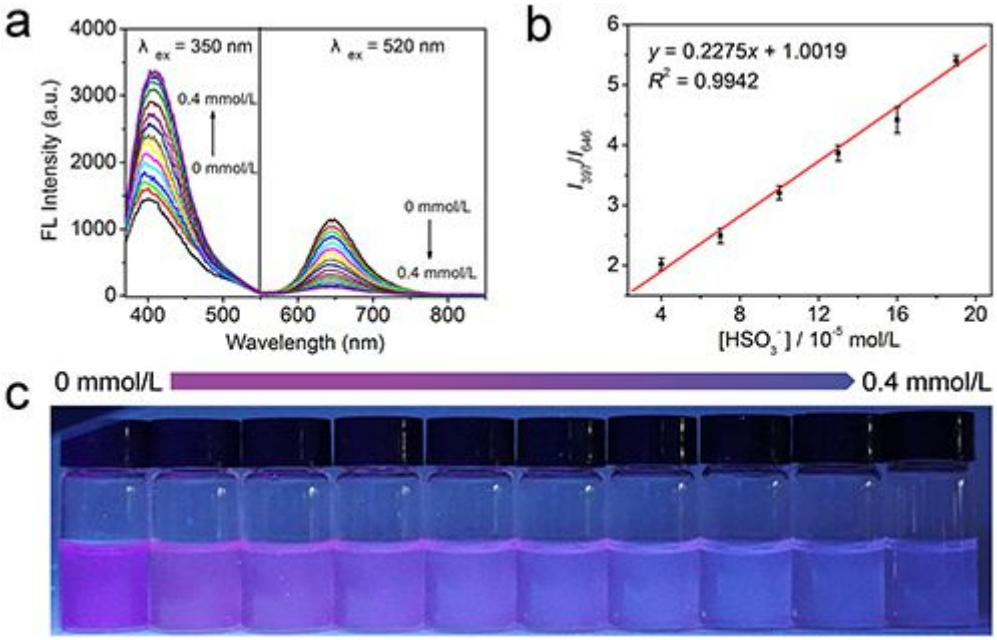

Figure 3

(a) Fluorescence spectra of probe PBI (1×10−5 M, Vwater:VDMSO = 8:2) with various concentrations of HSO3− (0 mmol/L−0.4 mmol/L). (b) I397/I646 as a function of different concentrations of HSO3− (0.04 mmol/L−0.19 mmol/L). (c) Photographs of PBI (1×10−5 M, Vwater:VDMSO = 8:2) in the different concentrations of HSO3− under Ultra violet lamp (365 nm).

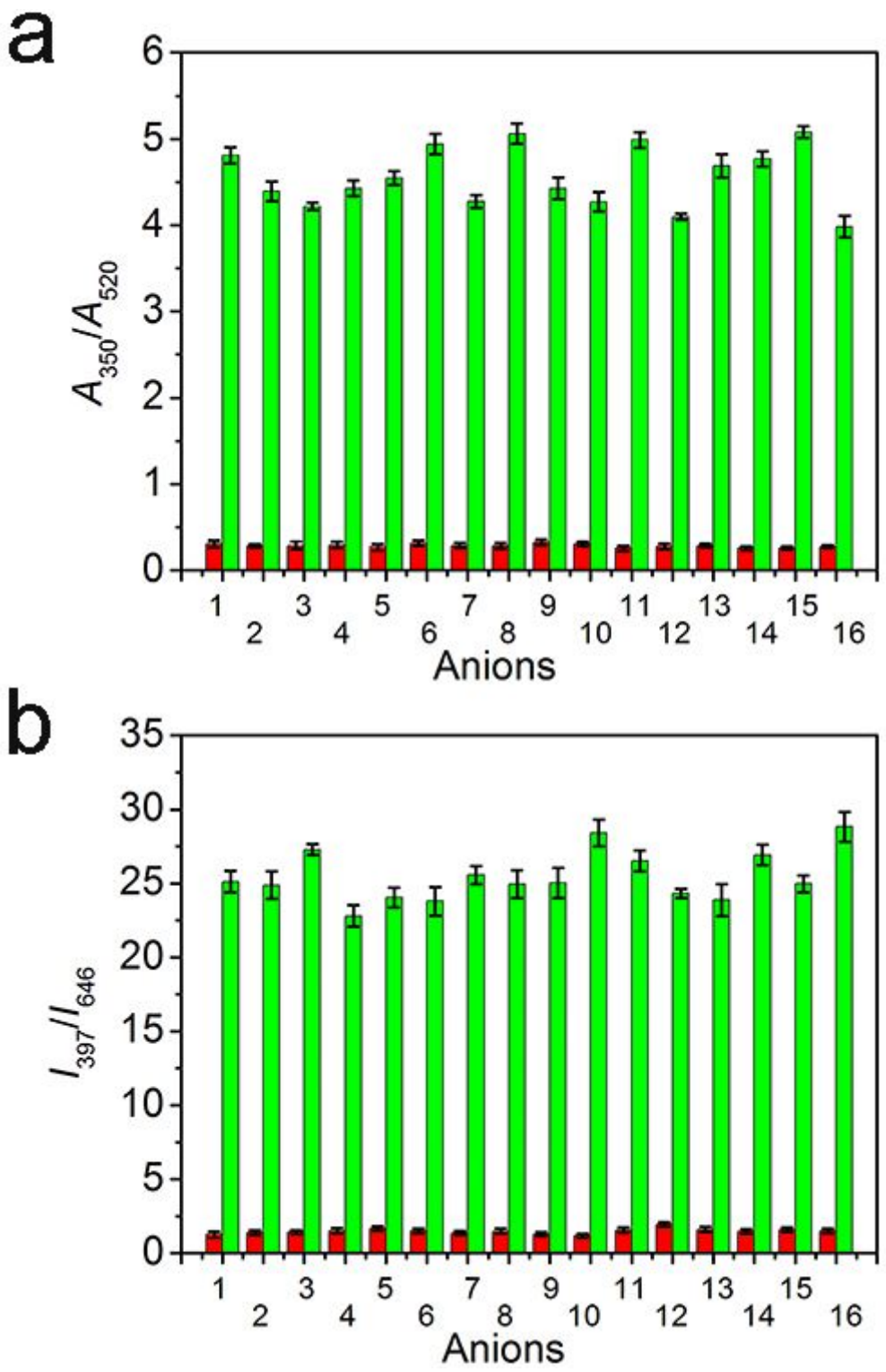

Figure 4

(a) A350/A520 of probe (1×10−5 M, Vwater:VDMSO = 8:2) with different anions (0.4 mmol/L). Red columns: different anions, green columns: HSO3− (0.4 mmol/L) and different anions (0.4 mmol/L). (b) I397/I646 of probe (1×10−5 M, Vwater:VDMSO = 8:2) with different anions (0.4 mmol/L). Red columns: different anions, green columns: HSO3− (0.4 mmol/L) and different anions (0.4 mmol/L). From left to right 1−16 respectively indicate: Blank, F−, Cl−, Br−, NO3−, NO2−, HSO4−, CO32−, ClO−, ClO3−, H2PO4−, HPO42−, PO43−, SCN−, BF4−, BrO3−.

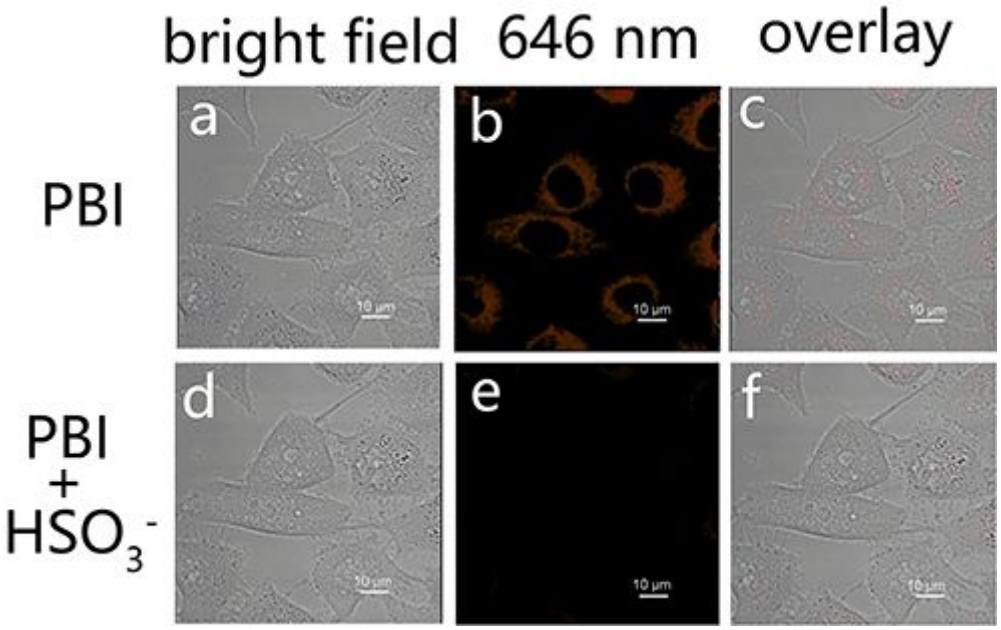

Figure 5

Fluorescence confocal images of probe PBI (1 μmol/L) to detect exogenous HSO3− (0.4 mmol/L) in HeLa cells. (a), (d): bright field images, (b), (e): images at 646 nm under 560 nm irradiation, (c), (f): overlay images.

Supplementary Files

This is a list of supplementary files associated with this preprint. Click to download.

- GraphicalAbstract.tif
- Scheme1.tif